LAPLACIAN OPERATORS FOR DIRECT PROCESSING OF RANGE DATA

[1]Sonya Coleman, [1]Shanmugalingam Suganthan, [2]Bryan Scotney

[1]School of Computing and Intelligent Systems, University of Ulster, Magee, BT48 7JL, Northern Ireland
[2]School of Computing and Information Engineering, University of Ulster, Coleraine, BT52 1SA, Northern Ireland

ABSTRACT

The use of range data has become prominent in the field of computer vision. Due to the irregular nature of range data that occurs with a number of sensors, feature extraction is a complex and challenging problem. Feature extraction techniques for range images are often based on scan line data approximations and hence do not employ exact data locations. We present a finite element based approach to the development of Laplacian operators that can be applied to both regularly or irregularly distributed range data. We demonstrate that the feature maps generated using our approach on range data are much less susceptible to noise than the traditional use of Laplacian operators on intensity images.

Index Terms— Range Images, Edge detection, Laplacian operators

1. INTRODUCTION

Range images are a special class of digital images in which each pixel value expresses the distance between a known reference frame and a visible point in the scene. A range image reproduces, therefore, an almost 3D representation of a scene [2]. Computer vision applications increasingly use range image data instead of, or in conjunction with, intensity image data [3]. Intensity images are of limited use in terms of estimation of surfaces, as pixel values are related to surface geometry only indirectly. Range images encode the position of surfaces directly, and therefore the shape of an object can be computed reasonably easily from range data.

In intensity images, features tend to be defined as discontinuities in the image intensity due to changes in scene structure, and such discontinuities are often detected using either first or second order derivative operators. When applying a second order derivative operator, a feature is determined as a zero-crossing, some examples of which are presented in [4,6,7]. The main problem encountered when using outputs of second order derivative operators is that the feature map is very susceptible to noise, as every zero-crossing in the output is used to represent a feature point.

The problem of edge detection when using range images is significantly different from that when using intensity images. There are two issues to consider when dealing with range data: the locational distribution of the data and the definition of an edge in a range image. We firstly overcome the data distribution problem by generating Laplacian operators that are shape adaptive, and hence can be applied directly to irregularly distributed data. With respect to defining an edge in a range image, this differs significantly from the case of an intensity image. Generally, in an intensity image, a change in intensity indicates an edge, the significance of which is determined by the gradient of the change. However, in a range image, a continuous change in range data implies an object surface, and hence an edge is signified by a change in gradient where two object surfaces meet. Hence the output generated when a Laplacian operator is applied has a significantly different meaning from the equivalent output generated using an intensity image and must be interpreted differently. The complementarity of range and intensity data is valuable in resolving ambiguities, and issues of interpretation need to be considered in order to derive the benefits of fusing range data and intensity data.

This paper presents a shape adaptive Laplacian operator for direct use on range data without any pre-processing requirements. An overview of the range image representation is presented in Section 2 with Section 3 describing the finite element framework employed. A brief overview of the 3×3 shape adaptive Laplacian operator implementation is described in Section 4. In Section 5 we demonstrate how the output differs from that achieved using an intensity image and hence illustrate how to determine features in range images using Laplacian operators. Comparative results using the Laplacian operators are presented in Section 6, and these demonstrate that Laplacian operators are less susceptible to noise when used with range data than with intensity images.

2. RANGE IMAGE REPRESENTATION

We consider a range image to be represented by a spatially irregular sample of values of a continuous function $u(x,y)$ of depth value on a domain Ω. Our operator design procedure is then based on the use of a quadrilateral mesh as illustrated in Figure 1 in which the nodes are the sample points.

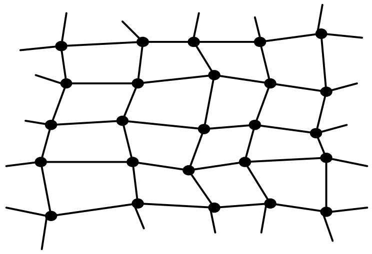

Figure 1. Sample of the irregularly distributed range image

With each node i in the mesh is associated a piecewise bilinear basis function $\phi_i(x,y)$ which has the properties $\phi_i(x_j, y_j) = 1$ if $i = j$ and $\phi_i(x_j, y_j) = 0$ if $i \neq j$, where (x_j, y_j) are the co-ordinates of the nodal point j in the mesh. Thus $\phi_i(x,y)$ is a "tent-shaped" function with support restricted to a small neighbourhood centred on node i consisting of only those elements that have node i as a vertex. We then approximately represent the range image function u by a function $U(x,y) = \sum_{j=1}^{N} U_j \phi_j(x,y)$ in which the parameters $\{U_1, ..., U_N\}$ are mapped from the range image pixel values at the N irregularly located nodal points. Therefore, approximate image representation is a simple function (typically a low order polynomial) on each element and has the sampled range value U_j at node j.

3. FINITE ELEMENT FRAMEWORK

In order to obtain the weak form of the Laplacian operator, it is necessary that the image function $u = u(x,y)$ is once differentiable in the sense of belonging to the Hilbert space $H^1(\Omega)$, i.e., the integral $\int_\Omega \left(|\underline{\nabla} u|^2 + u^2\right) d\Omega$ is finite, where $\underline{\nabla} u$ is the vector $(\partial u/\partial x, \partial u/\partial y)^T$ [1]. The Laplacian term $-\underline{\nabla} \cdot (\underline{\nabla} u)$ is multiplied by a test function $v \in H^1$ and the result is integrated on the domain Ω to give

$$R(u) = -\int_\Omega \underline{\nabla} \cdot (\underline{\nabla} u) v d\Omega \tag{1}$$

and this may be expanded to give

$$R(u) = \int_\Omega \underline{\nabla} u \cdot \underline{\nabla} v d\Omega - \int_\Omega \underline{\nabla} \cdot (\underline{\nabla} u v) d\Omega . \tag{2}$$

$$= \int_\Omega \underline{\nabla} u \cdot \underline{\nabla} v d\Omega - \int_{\partial\Omega} (\underline{\nabla} u v) \cdot \underline{n} d\Gamma \tag{3}$$

As the function space H^1 is infinite dimensional, we use the Galerkin formulation to obtain an approximate solution to a problem in a finite dimensional subspace $S^h(\Omega) \subset H^1(\Omega)$ rather than in the whole space $H^1(\Omega)$. Using the range image representation presented in Section 2, we may approximately represent the weak form of the Laplacian of the image by the functional

$$R_i(U) = \int_\Omega \underline{\nabla} U \cdot \underline{\nabla} \phi_i d\Omega - \int_{\partial\Omega} (\underline{\nabla} U \phi_i) \cdot \underline{n} d\Gamma \tag{4}$$

for each function ϕ_i in the basis S^h. The boundary term in equation (4) may be disregarded if ϕ_i is restricted to a local neighbourhood and has zero value on the image boundary. If the test functions ϕ_i used in the weak form functional are from the same space as those used in the image approximation, this formulation corresponds to the Galerkin method in finite element analysis. However, we use an alternative approach whereby a finite-dimensional test space T_σ^h is employed which differs from the image space S^h; such an approach corresponds to the Petrov-Galerkin finite element formulation. This leads to the representation of the Laplacian by the functional

$$R_i^\sigma(U) = \int_{\Omega_i^\sigma} \underline{\nabla} U \cdot \underline{\nabla} \psi_i^\sigma d\Omega_i \tag{5}$$

where ψ_i^σ is a test function from the test space T_σ^h, with support restricted to a neighbourhood Ω_i^σ of node i. In particular we choose ψ_i^σ to be a Gaussian test function with support restricted to a local neighbourhood of elements surrounding node i.

4. OPERATOR IMPLEMENTATION

To illustrate the implementation of the 3×3 Laplacian operator, we use a neighbourhood comprised of a set S_i^σ of four elements as illustrated in Figure 2. A Gaussian basis function ψ_i^σ is associated with the central node i and shares common support with nine neighbouring basis functions ϕ_j (including ϕ_i). Contributions to the operator $R_i^\sigma(U)$ therefore need to be computed over four elements.

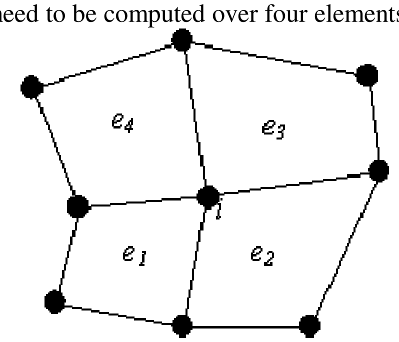

Figure 2. Local 3×3 operator neighbourhood

Substituting the image representation $U(x,y) = \sum_{j=1}^{N} U_j \phi_j(x,y)$ into the weak form in (5) yields

$$R_i^\sigma(U) = -\sum_{j=1}^{N} K_{ij}^\sigma U_j - \sum_{j=1}^{N} L_{ij}^\sigma U_j \tag{6}$$

where K_{ij}^σ and L_{ij}^σ are respectively entries in $N \times N$ global matrices K^σ and L^σ given by $K_{ij}^\sigma = \int_{\Omega_i^\sigma} \frac{\partial \phi_j}{\partial x} \frac{\partial \psi_i^\sigma}{\partial x} dxdy$, i,j=1,..,N and $L_{ij}^\sigma = \int_{\Omega_i^\sigma} \frac{\partial \phi_j}{\partial y} \frac{\partial \psi_i^\sigma}{\partial y} dxdy$, i,j=1,..,N. These integrals need to be computed only over the neighbourhood Ω_i^σ, rather than the entire image domain Ω, since ψ_i^σ has support restricted to Ω_i^σ.

The adaptive capabilities of the operators are enabled by element mapping. An irregular bilinear element is mapped onto a regular bilinear reference element, as illustrated in Figure 3; the corresponding co-ordinate transformation is defined as

$$x = \frac{1}{4}(x_1(1-\xi)(1-\eta) + x_2(1+\xi)(1-\eta) + x_3(1+\xi)(1+\eta) + x_4(1-\xi)(1+\eta)) \tag{7}$$

$$y = \frac{1}{4}(y_1(1-\xi)(1-\eta) + y_2(1+\xi)(1-\eta) + y_3(1+\xi)(1+\eta) + y_4(1-\xi)(1+\eta)) \tag{8}$$

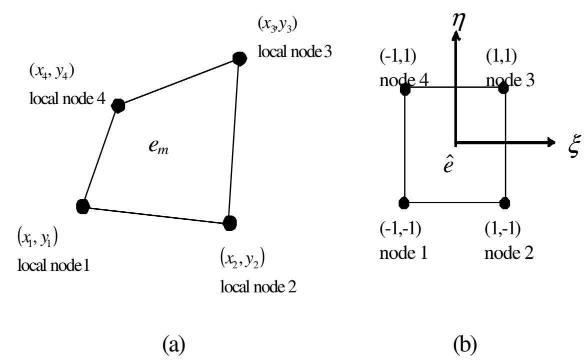

Figure 3. (a) Cartesian reference system for Bilinear element e_m (b) Bilinear reference element.

Construction of the operators on an irregular quadrilateral grid differs from that of image processing operators on a typically regular grid in that it is no longer appropriate to build explicitly an entire operator, as each operator throughout an irregular mesh may be different with respect to the operator neighbourhood shape. When using an irregular grid, we work on an element-by-element basis, taking advantage of the flexibility offered by the finite element method as a means of adaptively changing the irregular operator shape to encompass the data available in any local neighbourhood.

5. LAPLACIAN OUTPUT

We demonstrate how the Laplacian output when using a range image differs from that when an intensity image is used. Given the 1D signal in Figure 4(a), if this represented a ramp edge in an intensity image, the edge is distinguished in the Laplacian output as a zero-crossing as illustrated in Figure 4(b). However, if the 1D signal in Figure 4(a) corresponds to a section of a range image, each line segment in the signal is equivalent to an object surface. Therefore, each of the peaks in the Laplacian output, as illustrated in Figure 4b, represents an edge in a range image. Hence, features in range images can be found readily by computing the absolute value of the Laplacian output together with simple thresholding to ensure that only the most significant peaks are representative of edges. Thus the use of Laplacian operators for feature extraction in range images is less susceptible to noise than in intensity images

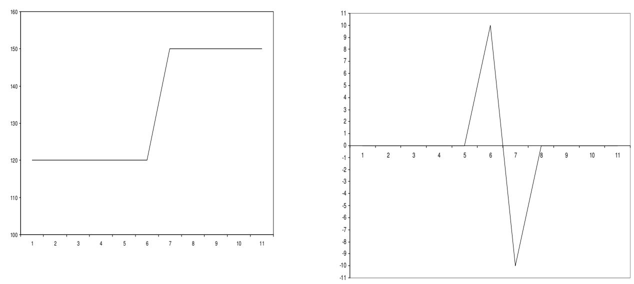

Figure 4. (a) 1D signal; (b) Laplacian response

6. RESULTS

To evaluate performance we compare our proposed technique with that of Jiang et al [5].

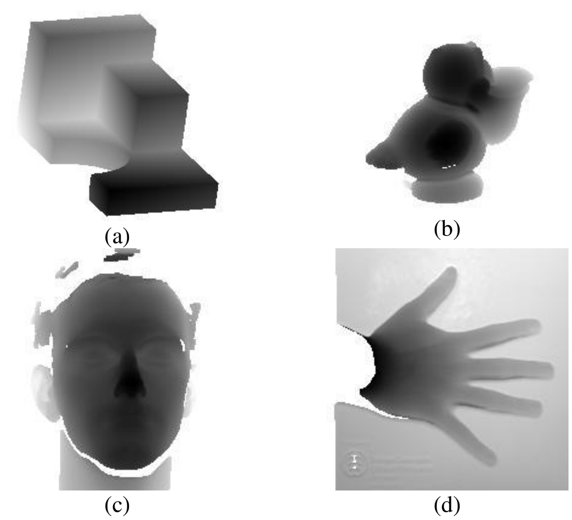

Figure 5. Original range images: (a) from the Technical Arts scanner; (b),(c),(d) from the Minolta 700 range scanner (http://marathon.csee.usf.edu/range/DataBase.html)

The algorithm in [5] is a scan line approximation approach that scans the image vertically, horizontally and diagonally. We illustrate our technique using four real images (Figure 5), but taken by two different range scanners: Technical Art scanner and OSU's Minolta 700 range scanner. The images captured using the Technical Arts scanner have regularly distributed data and those captured by the Minolta 700 range scanner have irregularly captured data, thus demonstrating that the proposed technique is not range sensor specific. Edge maps for both the proposed method and that in [5] are illustrated in Figure 6. It should be noted that our proposed technique automatically finds all features whereas the technique in [5] does not automatically find the object boundary via the scan line approximation but instead assumes the boundary at the transition between data and no data in the range image.

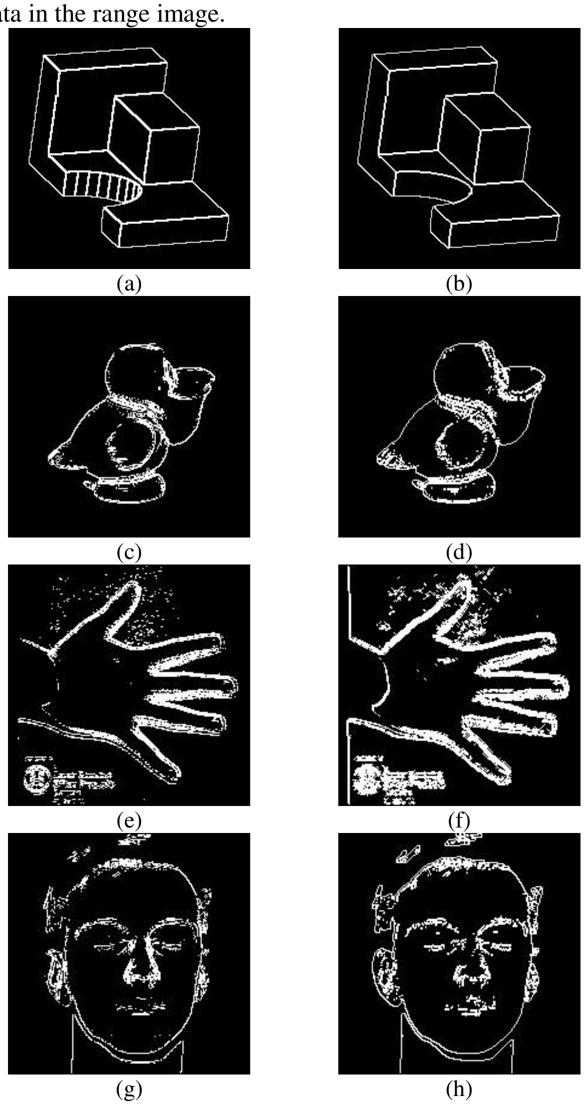

Figure 6. Edge map: (a), (c), (e), (g) edge maps generated using proposed technique; (b), (d), (f), (h) edge maps generated using scan line technique [5]

It can be seen from Figure 6 that our proposed technique provides edge maps that are comparable with those generated using the scan line approximation approach in [5]. In some cases our technique provides additional edge detail (Figure 6(a)) or finer edges (Figure 6(e)). It can also be seen from Figure 6 that the edge maps generated using the Laplacian operator are not as noisy as would typically be expected from the zero-crossing output when a Laplacian operator is applied to an intensity image.

7. SUMMARY AND FUTURE WORK

We have presented a shape adaptive 3×3 Laplacian operator that can be used directly on range image data without the need for any image pre-processing. Current results are promising when compared with the scan line approach of Jiang et al. [5]. Future work will involve generating irregular quadrilateral operators of varying size, not just 3×3, to enable multi-scale feature extraction. Also, these techniques will be evaluated with respect to existing edge based segmentation algorithms with the overall goal of recognizing objects in range images in real-time.

Acknowledgement
This work was supported by the U.K Research Council EPSRC under Grant EP/C006283/1. We would like to thank Prof. Horst Bunke for providing us with the code for the scan line approximation algorithm in [5]

8. REFERENCES

[1] Becker, E.B., Carey, G.F., Oden, J.T., "Finite Elements: An Introduction." Prentice Hall, London, 1981
[2]Besl, P.J., "Active, optical range imaging sensors", Machine Vision and Apps, Vol.1, pp. 127-152, 1988.
[3] Dias, P., et al., "Combining Intensity and Range Images for 3D Modelling", Proceedings of the IEEE International Conference on Image Processing (ICIP2003).
[4] Haralick, R.M., "Zero crossing of second directional derivative edge operator", in Proc. SPIE Symp. Robot Vision, Vol.336, Washington, DC, pp.91-99, 1982
[5] Jiang X. Y., Bunke H. "Edge detection in range image based on scan line approximation" Computer Vision and Image Understanding 73(2), 183-199, 1999
[6] Kimmel R., and Bruckstein, A.M., "Regularized Laplacian Zero Crossings as Optimal Edge Integrators", International Journal of Computer Vision 53(3), 225-243, 2003
[7] Marr D., Hildreth, E., "Theory of edge detection", Proc. Roy. Soc., vol. B207, pp.187-217, 1980